

# PHYS 453 Lab Report: Optical Pumping

Michael Jafs<sup>1,\*</sup>

<sup>1</sup>*Department of Physics, Engineering Physics and Astronomy,  
Queen's University, Kingston, ON K7L 3N6, Canada*

(Dated: March 1, 2022)

Optical pumping is a versatile technique which uses a polarized light source to manipulate atoms to a specific spin state. In this lab, we consider <sup>85</sup>Rb and <sup>87</sup>Rb and explore first the splitting of the energy levels in the presence of a magnetic field - the Zeeman Effect, and identify the location for which the linear Zeeman Effect becomes quadratic. We find this to be when the magnetic field has a strength of roughly 5 Gauss. We then solve the rate equations for the populating of states in <sup>87</sup>Rb and explore the solutions when considering only the  $D_1$  transition. We find that our numerical simulations are incorrect and thus produce a plot which has little physical meaning. We identify why our results do not make sense and provide motivation for what might be the cause of our errors.

## I. INTRODUCTION

In optical pumping, atoms within a given element are manipulated by a light source into a certain spin state. Essentially, a photon is able to excite an electron to a specific sub-level, however, the average decay results in a “pumped” state where more atoms are oriented with the same spin state. This can be particularly useful in science since there are many applications in which one may want to at some point in a procedure, polarize a gas. The Nobel prize was even awarded for the technique in 1966 [1].

In this lab, we consider the effects of optically pumping both <sup>85</sup>Rb and <sup>87</sup>Rb using radio-frequency (RF) polarized light. In Section II, we outline the theory and necessary background to understand how one could optically pump an atom into a specific spin state. We proceed by exploring the onset of the linear and quadratic Zeeman Effect in Section III, and summarize the results of a numerical simulation of optical pumping in Section IV. Finally, we provide concluding remarks in Section V.

## II. BACKGROUND AND THEORY

The following discussion closely follows the development of the theory of optical pumping found in [1]. In doing so, we must consider first the basic theory of atomic structure, photon absorption, and light polarization to better outline the rationale behind optical pumping.

When we consider atomic structure, we typically consider energy levels within an atom, that possess corrections at smaller energy scales, such that the splitting between the corrections themselves is much less than the splitting of the initial energy levels. This structure begins with electron structure in which the energy levels describe orbitals for which electrons reside within the atom. The orbitals are described by a number  $n$  denoting the energy level and orbital size, and a letter which represents the angular momentum of the orbital shell. The electronic configuration for Rb is:

$$1s^2 2s^2 2p^6 3s^2 3p^6 3d^{10} 4s^2 4p^6 5s^1 \quad (1)$$

With a further refinement, we reach what is known as “fine structure” which takes into account the fact that electrons themselves have spin,  $S = 1/2$  and consequently a dipole moment. This spin orbit coupling is a result of the electron interacting with the positively charged nucleus and shifts the energy slightly. The interaction term in the Hamiltonian takes the form  $\mathbf{L} \cdot \mathbf{S}$  and we define a new quantum number  $\mathbf{J} = \mathbf{L} + \mathbf{S}$  which represents the total angular momentum of the shell and can take integer values so that  $|L - S| \leq J \leq L + S$ . Fine structure is on the order of a few THz.

If we consider the fact that the nucleus has a spin also, we reach what is known as “hyperfine structure”. We denote the nuclear spin with the letter  $I$  which couples to  $J$  leading to the term  $\mathbf{J} \cdot \mathbf{I}$  in the Hamiltonian. We also define the new quantum number  $\mathbf{F} = \mathbf{J} + \mathbf{I}$  which similarly obeys  $|J - I| \leq F \leq J + I$ . Hyperfine structure plays a role when we consider isotopes of the same element since the number of neutrons and consequently nuclear spin will be different. Therefore each isotope of the same element has a different hyperfine structure.

Going a step further, we note that in the presence of a magnetic field, the  $2F+1$  degenerate hyperfine levels become non-degenerate as the magnetic dipole moment of the atom interacts with the magnetic field. This is known as the Zeeman effect, where for small magnetic fields, the unperturbed energy level  $E_z$  is related to the Zeeman levels  $M_F$  through,

$$E_z = g_F \mu_B B M_F \quad (2)$$

where expressions for  $g_F$  and  $g_J$  are given in [1] and  $\mu_B$  is the Bohr magneton. Eq. 2 is linear with respect to perturbed and unperturbed levels, however, this is only true for small magnetic fields, since one could in theory boost  $B$ , so that the right hand side of 2 becomes bigger than  $E_z$ .

Photon absorption takes place when a photon incident on an atom has energy  $E = h\nu$  equal to the energy required to excite the atom to a higher energy state. The transition we care about for the purposes of this investigation is the electric dipole transition, for which selection rules state that the following must be satisfied:

$$\Delta F = 0, \pm 1 \quad \& \quad \Delta M_F = 0, \pm 1, \quad (3)$$

---

\* 17msj2@queensu.ca

which is only misleading in the sense that we also cannot have the transition  $F = 0 \rightarrow F = 0$ . If the incident light beam is not of sufficient intensity, transitions between different  $F$  levels will not take place, and the specific transition between Zeeman levels depends on how the light is polarized.

Three polarization types are necessary to consider here: linear, right-circular (RCP), and left-circular (LCP). They each differ by a relative phase difference between the electric and magnetic components of the E&M wave. For linear polarization, the phase difference is zero. For left and right circular polarization, the phase difference is  $\pi/2$  with one of the components “lagging” behind the other. To achieve optical pumping, we require that the light be either RCP or LCP, since these correspond to the transitions  $\Delta M_F = 1$  and  $\Delta M_F = -1$  respectively.

### A. Optical Pumping

For the purposes of this investigation, we consider only optical light that drives the transition from the  $^2S_{1/2}$  fine level to the same hyperfine level in the  $^2P_{1/2}$  state. The  $D_1$  transition. The key here is that, using either RCP or LCP, the electron will be excited to a higher (or lower) energy level by the incident light, even though the average de-excitation will be of the kind  $\Delta M_F = 0$ . Therefore the atom will be pumped into the ground state with either the highest (or lowest)  $M_F$  depending on the choice of RCP or LCP light.

## III. ENERGY LEVELS IN AN EXTERNAL MAGNETIC FIELD

Since this lab was carried out online, our tasks only consisted of simulations and numerical modelling. It is for this reason that we do not describe an experimental procedure or apparatus but rather outline our steps taken while developing our numerical model and how we simulated our results.

### A. Eigen-energies

We began by simulating the effects of the Zeeman splitting outlined in Section II. Fundamentally, we are required to solve the time-independent Schrödinger equation (TISE):

$$\hat{H}|\psi\rangle = E|\psi\rangle, \quad (4)$$

for which  $\hat{H}$  is the Hamiltonian operator,  $E$  is the energy eigen-value and  $|\psi\rangle$  is the corresponding energy eigenvector. In its ground state, we can write the Hamiltonian operator for Rb as:

$$\hat{H} = \hat{H}_B + \hat{H}_{hf} \quad (5)$$

which only takes into account  $\hat{H}_B$ : the interaction between the atom and the magnetic field, and  $\hat{H}_{hf}$ : the interaction between the nucleus and the electron. The hyperfine interaction term takes the form:

$$\hat{H}_{hf} = a_{hf} \mathbf{S} \cdot \mathbf{I} = a_{hf} (\hat{S}_x \hat{I}_x + \hat{S}_y \hat{I}_y + \hat{S}_z \hat{I}_z) \quad (6)$$

where  $a_{hf}$ , the hyperfine interaction constant, is equal to  $h \cdot 1.011$  GHz for  $^{85}\text{Rb}$  [2] and  $h \cdot 3.417$  GHz for  $^{87}\text{Rb}$  [3].

If we take  $B = B_0 \hat{z}$ , then the atomic interaction term takes the form:

$$\begin{aligned} \hat{H}_B &= \frac{\mu_B}{\hbar} (g_S \mathbf{S} + g_I \mathbf{I}) \cdot \vec{B} \\ &= \frac{\mu_B}{\hbar} (g_S \hat{S}_z + G_I \hat{I}_z) B_0. \end{aligned} \quad (7)$$

With the choice of basis states  $|S, m_s\rangle$  and  $|I, m_I\rangle$  with the tensor product yielding  $|m_s, m_I\rangle$ . The matrix elements of  $\hat{H}_B$  are then given by:

$$\langle m'_s, m'_I | \hat{H}_B | m_s, m_I \rangle = \mu_B B_0 (g_S m_s + g_I m_I) \delta_{m_s, m'_s} \delta_{m_I, m'_I}. \quad (8)$$

Where the electron spin g-factor  $g_S = 2.002319$  and the nuclear g-factors are  $g_I = -0.000995$  for  $^{87}\text{Rb}$  and  $G_I = -0.000293$  for  $^{85}\text{Rb}$  [2, 3]. Similarly, the hyperfine interaction term can be re-written as:

$$\hat{H}_{hf} = a_{hf} \left( \frac{1}{2} (S_+ I_- + S_- I_+) + \hat{S}_z \hat{I}_z \right), \quad (9)$$

using the definitions for  $S_x$  and  $S_y$ . It is then straight forward to construct expressions for the matrix elements of  $\hat{H}_{hf}$  which can be found in [1].

Using these results, we were able to construct the full  $\hat{H}$  matrix for both rubidium 85 and 87. Since  $I = 3/2$  for  $^{87}\text{Rb}$  and  $I = 5/2$  for  $^{85}\text{Rb}$  [1, 2] we can determine values of  $m_s$  and  $m_I$  for each of the rubidium isotopes. After constructing the full Hamiltonian matrices and diagonalizing them using the `numpy.linalg.eig` package within python, we were able to achieve values for the eigen-energies at specific values of the magnetic field  $B$ .

Figure 1 shows the functional dependence that the eigen-energies have on the the magnetic field strength. It is clear that when no external field is applied to the atom, or  $\vec{B} = 0$ , two possible energy levels exist at the hyperfine level for the ground state of each isotope. Therefore, as we increase  $B$ , we expect the splitting of each of these degenerate levels corresponding to the respective  $M_F$  possible values. In other words, we are seeing a Zeeman splitting for each atom. We can also see that for large values of  $B$ , the splitting for many values of  $M_F$  becomes non-linear. This is the large field regime which we will discuss in further depth in the following section.

### B. RF Transition Frequencies

To construct the transition frequencies, we calculated and plotted the difference between successive lines for both  $^{85}\text{Rb}$  and  $^{87}\text{Rb}$  in Figure 1. The transition frequencies,

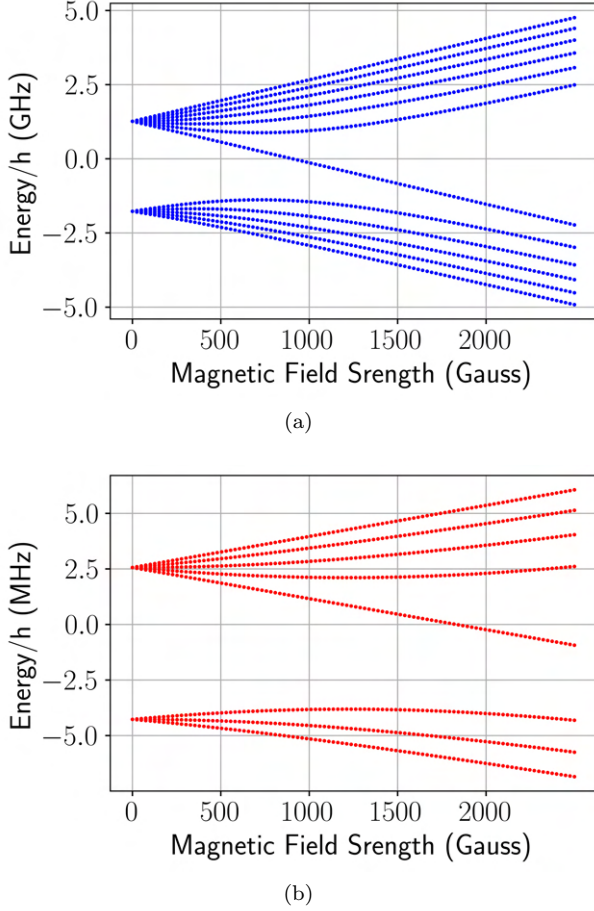


Figure 1. Eigen-energies as a function of magnetic field strength for both  $^{85}\text{Rb}$  and  $^{87}\text{Rb}$ . (a) corresponds to  $^{85}\text{Rb}$ . (b) corresponds to  $^{87}\text{Rb}$ .

expressed as energies, are plotted in Figure 2. We expect there to be 6 distinct resonances corresponding to  $^{85}\text{Rb}$  and 4 distinct resonances for  $^{87}\text{Rb}$ . This is due to the fact that we have at most 6 unique splittings for  $^{85}\text{Rb}$  and 4 for  $^{87}\text{Rb}$  and is precisely what we found by constructing the transition frequencies in Figure 2. It is clear that up to a certain magnetic field strength, the energy eigen-values in Figure 1 follow a linear trend that eventually seems to diverge quadratically. The same can be said for our plot of the transition frequencies. Since the linear equation we wrote down describing the Zeeman Effect (E. 2) only applies to the small field regime, we expect that when the applied field is small, the transition frequencies will be equal.

In Figure ??, we plot the transition frequencies for  $^{87}\text{Rb}$  for only the first 10 Gauss. It is clear from this figure, that the location in which the transition frequencies begin to become non-degenerate, is roughly 5.0 Gauss. Therefore, we can conclude that the small field regime, and therefore the linear Zeeman Effect, is only true for an applied magnetic field of less than 5.0G.

#### IV. SIMULATION OF OPTICAL PUMPING

In this section, we discuss the results of our numerical modelling of the  $D_1$  transition in  $^{87}\text{Rb}$  and our simulation

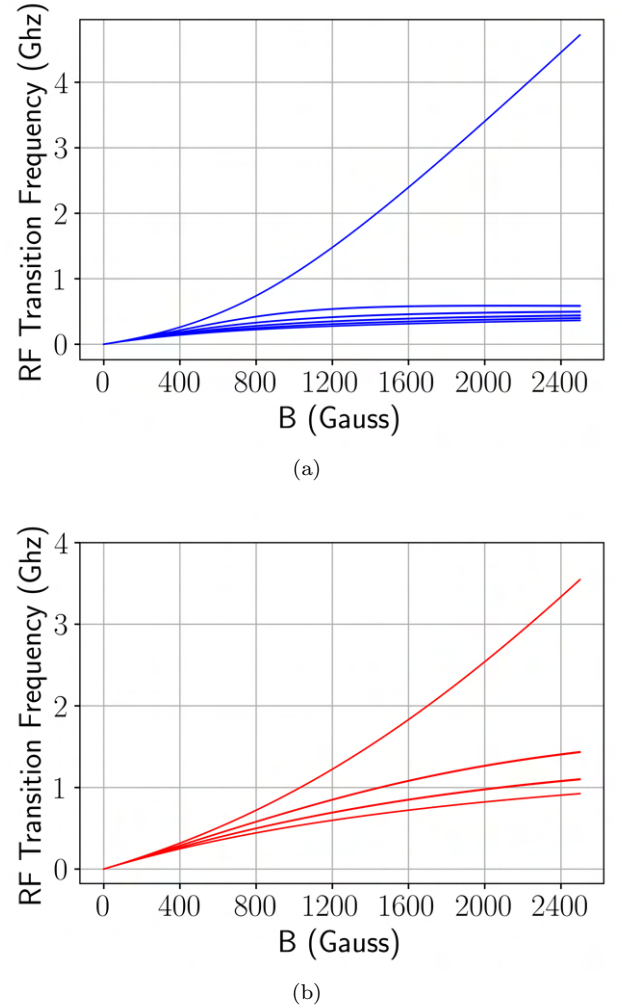


Figure 2. Transition frequencies as a function of magnetic field strength for both  $^{85}\text{Rb}$  and  $^{87}\text{Rb}$ . (a) corresponds to  $^{85}\text{Rb}$ . (b) corresponds to  $^{87}\text{Rb}$ .

of optical pumping. We decided to label the ground state sub-levels with the index  $k$ , and the excited state levels with the index  $i$ , so that the rate equations took the form:

$$\begin{aligned}\dot{K}_k &= \sum_i P_{ik}(N_i - N_k) + \sum_i \Gamma_{ik}N_i \\ \dot{K}_i &= \sum_k P_{ik}(N_k - N_i) + \sum_k \Gamma_{ik}N_i\end{aligned}\quad (10)$$

Therefore, in order to determine the amount of atoms in an excited, or ground state after some time  $t$ , we simply were required to solve the system of 16 coupled ode's seen in Eq. 10. Full expressions for the matrices  $P_{ik}$  and  $\Gamma_{ik}$  can be found in [1]. Setting our initial conditions such that  $N_k = 1/8 \forall k$  and  $N_i = 0 \forall i$ , for a total simulation time of  $2.0 \times 10^{-6}$  seconds, are results can be seen in Figure 4. Unfortunately, there are a number of issues with Figure 4 which are likely the result of a computational error during our simulation. We have attempted to solve the system of equations 10, using a 4th-order Runge Kutta algorithm subroutine. At first glance, our initial conditions are not satisfying on the plot since it appears as though both pop-

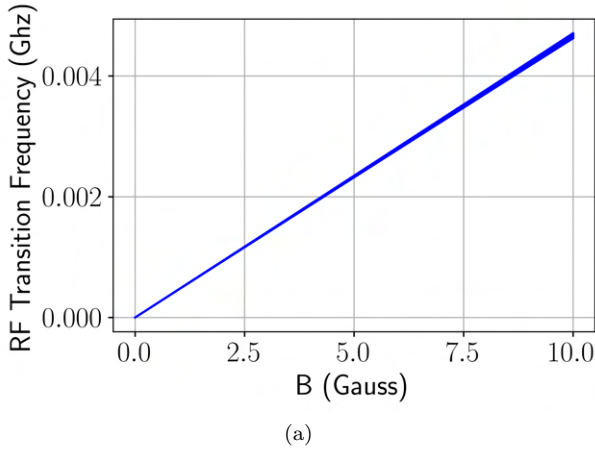


Figure 3. Transition frequencies for  $^{87}\text{Rb}$  as a function of magnetic field strength up to only 10 Gauss.

ulations are beginning with a value of zero. However, our scaling is very large on the y-axis and so it is more likely that we simply cannot recognize the difference between such small values of  $1/8$  and  $0$ . Second, the shape of the plot is non-sensical, and the figure implies that the population quickly takes on negative values as time moves forward which is simply not possible. Therefore, we conclude that our numerical modelling process itself was insufficient for solving the rate equations (Eq. 10) and determining the population of states over time.

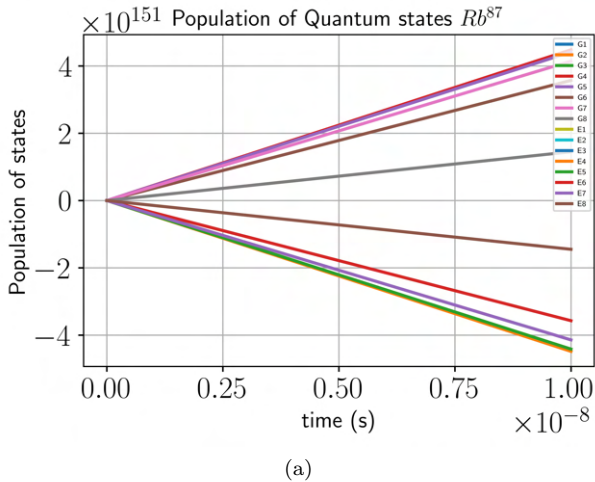


Figure 4. Population of states corresponding to the simulation of optically pumping  $^{87}\text{Rb}$  using left polarized ( $\Delta M_F$ ) light. We consider only the  $D_1$  transition.

## V. CONCLUSIONS

We outlined the basic theoretical approach to understanding optical pumping by first building up the perturbative picture of energy levels within an atom. By describing photon absorption and the kind of light polarization necessary for optical pumping, we were able to outline the theory behind optical pumping itself. If one takes light to

be RCP, then by using a RF light source, one can excite an atom in the  $D_1$  transition. The subsequent decay of the atom will have an average transition between Zeeman levels of  $M_F = 0$  meaning over time, the atom will end up in a pumped state. We then explored the onset of the linear and quadratic Zeeman effect and found that by numerically simulating the effects of  $^{85}\text{Rb}$  and  $^{87}\text{Rb}$  in the presence of an applied magnetic field, the traditional linear Zeeman Effect only held for roughly less than  $B = 10$  Gauss. For magnetic fields beyond this value, we enter what is known as the strong field regime. We simulated the effects of optically pumping  $^{87}\text{Rb}$  by simulating the  $D_1$  transition with a LCP light source. We found that our numerical model was incorrect since we were not able to produce a viable plot. We found that the scaling of the vertical axis was extremely large, and that our simulation implied that the population of states could take on negative values for later times. This does not make sense since the definition of the population is by construction a value greater than or equal to zero. If given more time, we would have liked to investigate further the cause for these numerical errors and explore more deeply the effects of optically pumping  $^{87}\text{Rb}$  with LCP light.

## ACKNOWLEDGMENTS

Thank you to Madison Reed, Merlyn John, and Anika Chowdury for each helping with the numerical simulations and plotting the results found throughout this report.

## Appendix A: Executive Summary

In optical pumping, atoms within a given element are manipulated by a light source into a certain spin state. Essentially, a photon is able to excite an electron to a specific sub-level, however, the average decay results in a “pumped” state where more atoms are oriented with the same spin state. This can be particularly useful in science since there are many applications in which one may want to at some point in a procedure, polarize a gas. The Nobel prize was even awarded for the the technique in 1966 [1].

For the purposes of this investigation, we consider only optical light that drives the transition from the  $^2S_{1/2}$  fine level to the same hyperfine level in the  $^2P_{1/2}$  state. The  $D_1$  transition. The key here is that, using either RCP or LCP, the electron will be excited to a higher (or lower) energy level by the incident light, even though the average de-excitation will be of the kind  $\Delta M_F = 0$ . Therefore the atom will be pumped into the ground state with either the highest (or lowest)  $M_F$  depending on the choice of RCP or LCP light.

Figure 5 shows the functional dependence that the eigen-energies have on the the magnetic field strength. It is clear that when no external field is applied to the atom, or  $\vec{B} = 0$ , two possible energy levels exist at the hyperfine level for the ground state of each isotope. Therefore, as we increase  $B$ , we expect the splitting of each of these degenerate levels corresponding to the respective  $M_F$  possible values. In other words, we are seeing a Zeeman splitting for each atom. We can also see that for large values of  $B$ , the splitting for many values of  $M_F$  becomes non-linear.

This is the large field regime which appears to be at quite low magnetic field strength. We found that actually, the onset of the quadratic Zeeman effect occurred when the magnetic field strength was roughly 5 Gauss.

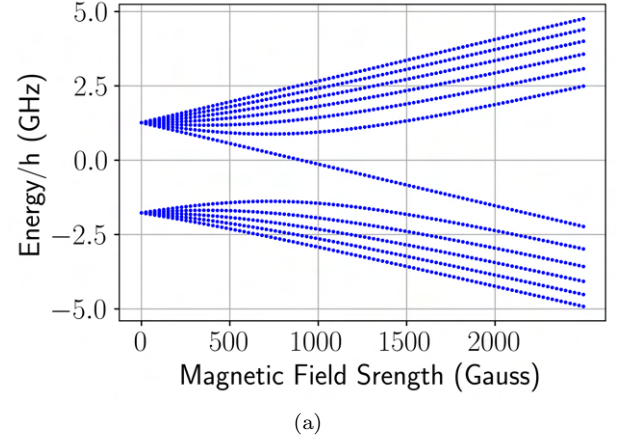


Figure 5. Eigen-energies as a function of magnetic field strength for  $^{85}\text{Rb}$  displaying both the linear and quadratic Zeeman Effect.

## References

- [1] J-M Nunzi, “Phys 453-advanced physics laboratory optical pumping experiment,” (2022).
- [2] Daniel Adam Steck, “[Rubidium 85 d line data](#),” (2008).
- [3] Daniel Adam Steck, “[Rubidium 87 d line data](#),” (2001).